scientific reports

Check for updates

OPEN

JAML overexpressed in colorectal cancer promotes tumour proliferation by activating the PI3K-AKT-mTOR signalling pathway

Yuying Fang[1,2,3,8], Yanan Liu[1,2,3,8], Zhilin Dong[1,4], Xinchao Zhao[1,4], Mingyan Zhang[1,3], Yawen Zheng[1], Chunsheng Yang[1], Yufeng Wang[2,3], Ning Liu[1], Peng Yan[1], Yuan Ma[5], Fei Yang[5], Yan Zheng[6], Wencheng Zhang[7], Jianmin Yang[7] & Meili Sun[1,2]✉

The expression and biological function of junctional adhesion molecule-like protein (JAML) in colorectal cancer (CRC) remain unclear. Paraffin tissue samples from 50 cases of CRC were collected to determine the expression of JAML. JAML was overexpressed or knock-down in CRC cells to evaluated the proliferation, migration and invasion in vitro and in vivo. Western-blot and others were applied to explore the mechanisms. The study showed that JAML was highly expressed within cancer tissues in 50% (25/50) of patients with CRC, and was correlated with higher TNM stage ($p < 0.05$). Patients of JAML^{-high} group had poorer overall survival compared to JAML^{-low} group ($p = 0.0362$, HR = 0.4295, 95% CI of 0.1908–0.9667). The tumour infiltrating lymphocytes (TILs) was lower in the JAML^{-high} group than in the JAML^{-low} group ($p < 0.05$). Overexpression of JAML promoted the proliferation, migration, and invasion of CRC by activating the PI3K-AKT-mTOR signalling pathway both in vitro and in vivo. TILs were reduced in JAML^{-high} tumour tissues by decreasing chemokines such as CCL20 and CXCL9/10/11. Our study identified JAML, a potentially ideal target that is specifically highly expressed in CRC tissues, which promoted tumour proliferation, impaired T-lymphocytes infiltration, provided a promising therapeutic strategy for patients with CRC.

Keywords Junctional adhesion molecule-like protein (JAML), Colorectal cancer, Proliferation, Targeted therapy, T-cell infiltration

Colorectal cancer (CRC) seriously affects human health; among all cancers, CRC has the second highest incidence and third highest mortality in the world[1,2]. Currently, most patients with metastatic colorectal cancer (mCRC) who receive a combination of targeted therapy and chemotherapy have a survival of 24–36 months[3–6]. The mainly strategies of targeted therapy are antiangiogenesis and anti-EGFR antibody, and the survival benefits have achieved the platform for patients with mCRC[7]. Pembrolizumab has been supported as a first-line therapy in patients with microsatellite instability-high (MSI-H)/deficient mismatch repair (dMMR) mCRC, yielding a median overall survival (OS) time above 36.7 months in Keynote 177 patients[8]. However, patients with

[1]Department of Oncology, Central Hospital Affiliated to Shandong First Medical University, Jinan 250013, Shandong, People's Republic of China. [2]Department of Oncology, Jinan Central Hospital, Shandong University, Jinan 250013, Shandong, People's Republic of China. [3]Research Center of Translational Medicine, Laboratory Animal Center, Central Hospital Affiliated to Shandong First Medical University, Jinan 250013, Shandong, People's Republic of China. [4]Department of Clinical Medicine, Shandong First Medical University, Jinan 271016, Shandong, People's Republic of China. [5]Department of Pathology, Central Hospital Affiliated to Shandong First Medical University, Jinan 250013, Shandong, People's Republic of China. [6]Research Center of Translational Medicine, Central Hospital Affiliated to Shandong First Medical University, Jinan 250013, Shandong, People's Republic of China. [7]National Key Laboratory for Innovation and Transformation of Luobing Theory, The Key Laboratory of Cardiovascular Remodeling and Function Research, Chinese Ministry of Education, Chinese National Health Commission and Chinese Academy of Medical Sciences, Department of Cardiology, Qilu Hospital of Shandong University, Jinan 250012, People's Republic of China. [8]These authors contributed equally to this work. ✉email: smli1980@163.com

mismatch repair-proficient (pMMR) tumours, which account for 95% of mCRC cases, show few benefits from immunotherapy[9,10]. Therefore, new therapeutic strategies are urgently needed to improve the survival of patients with mCRC.

Junctional adhesion molecule-like protein (JAML), a member of the JAMs family, was first discovered in 2003 during the differentiation of myeloid leukaemia cells[11] and is a secreted type I transmembrane protein. Initial studies have shown that JAML is mainly expressed by a variety of innate and adaptive immune cells, such as neutrophils, monocytes, and T cells[12,13]. JAML mediates the adhesion and migration of various immune and endothelial/epithelial cells, thereby regulating the inflammatory response. Our research group was the first to find that JAML was highly expressed in gastric cancer tissues and was also associated with poor prognosis[14]. Subsequently, Wu reported high expression of JAML in patients with lung adenocarcinoma[15]. However, the expression and the biological function of JAML in CRC remain unclear.

Herein, we investigated the expression of JAML in patients with CRC, explored the role and regulatory mechanism of JAML in the biological behaviour of malignant tumours.

Results

High expression of JAML was correlated with late TNM stage in patients with CRC, accompanied by decreased T-cell infiltration and poor prognosis

The expression of JAML in 50 CRC patients was detected using immunohistochemistry, and the relationships between JAML expression and clinicopathological parameters were also analysed. Of the 50 patients, 28 (56%) were male and 22 (44%) were female. The patients ranged in age from 41 to 88 years (median age 66.5 years); 34 patients were ≥ 60 years (68%), and 6 patients were < 60 years (32%). JAML was stained brown-yellow and was expressed mainly in the cytoplasm and cell membrane of cancer cells, with a small amount of expression in interstitial immune cells and almost no expression in normal intestinal gland cells adjacent to cancer cells (Fig. 1A). The IHC result was the product of the stained area and intensity fractions. A score less than or equal to three indicated no expression, a score greater than or equal to four indicated expression, a score less than or equal to six indicated low expression, and a score greater than or equal to eight indicated high expression. IHC analysis revealed that JAML was highly expressed in 50% (25/50) of cancer tissues, while lowly experssed in 92% (46/50) of adjacent tissues (4 was the cut-off value for IHC results) ($p < 0.0001$) (Fig. 1B). Subsequently, we studied the relationship between JAML in CRC and various CRC pathological parameters. We found that JAML was highly expressed in patients with lymph node metastasis [81% (17/21) of patients with lymph node metastasis *vs.* 27.6% (8/29) of patients without lymph node metastasis ($p < 0.001$) and late TNM stage ($p < 0.0001$)] (Table 1).

We examined the relationship between JAML expression and tumour-infiltrating lymphocytes in CRC tissues. We found that high expression of JAML was often accompanied by decreased infiltration of $CD3^+$T cells; that is, the density of tumour-infiltrating $CD3^+$T cells in the $JAML^{-high}$ group was lower than that in the $JAML^{-low}$ group (Fig. 1C,D). We further determined the proportions of $CD4^+$, $CD8^+$ and $Foxp3^+$T-lymphocytes within the two groups. We found that the density of $CD8^+$T-lymphocytes infiltration in the $JAML^{-high}$ group was lower than that in the $JAML^{-low}$ group ($p < 0.05$); however, there was no significant difference in the distribution of $CD4^+$T and $Foxp3^+$ T-lymphocytes between the two groups (Fig. 1E–G).

Patients in the $JAML^{-high}$ group had shorter overall survival than those in the in the $JAML^{-low}$ group ($p = 0.0362$, HR = 0.4295, 95% CI of 0.1908–0.9667) (Fig. 1H). Further survival analysis showed that the survival rate in the $JAML^{-high}$ $CD3^{-low}$ group was significantly lower than that in the $JAML^{-low}$ $CD3^{-high}$ group ($p = 0.0003$, HR = 0.1106, 95% CI = 0.03794–0.3224) (Fig. 1I). Mortality risk ratio analysis revealed that the expression of JAML, higher TNM stage and regional lymph node metastasis predicted poor prognosis (HR > 1, $p < 0.05$), and the expression of CD3 and CD8 predicted a better prognosis (HR < 1, $p < 0.05$) (Fig. 2A).

JAML promoted the proliferation, migration, and invasion of CRC cells in vitro

We speculated that the expression of JAML in CRC may affect the malignant biological behaviour of tumour cells. First, we examined the expression of JAML in CRC cell lines (HCT116, LOVO, DLD-1, SW480, and SW620) and colorectal epithelial cells (NCM460) (Fig. 3A,B). Compared with that in NCM460 cells, the expression of JAML in LOVO, DLD-1, SW480, and SW620 cells was greater, while its expression was relatively lower in DLD-1 and SW480 cells than in HCT116 and LOVO cells. Therefore, we transfected the JAML plasmid into DLD-1 and SW480 cells to increase JAML expression. Western blot analysis also showed that the expression of JAML in DLD-1 and SW480 cells was significantly upregulated after transfection with the JAML plasmid (Fig. 3C,D). A lentivirus (shJAML) was used to transfect HCT116 and LOVO cells to reduce JAML expression (Fig. 3E,F). We obtained DLD-1 and SW480 cells with increased JAML expression and HCT116 and LOVO cells with low JAML expression.

We then performed cell migration, invasion, and proliferation experiments to verify the effect of JAML on the malignant behaviour of tumour cells. Transwell migration and invasion experiments showed that overexpression of JAML significantly increased the migration and invasion of DLD-1 and SW480 cells (Fig. 3G,H,J,K), whereas low expression of JAML decreased the migration and invasion abilities of HCT116 and LOVO cells (Fig. 3G,I,J,L). The results of the EdU proliferation assay ultimately showed that the overexpression of JAML significantly increased the proliferative ability of DLD-1 and SW480 cells (Fig. 3M,N), while the low expression of JAML decreased the proliferative ability of HCT116 and LOVO cells (Fig. 3M,O). Taken together, these results suggested that JAML promoted the proliferation, migration, and invasion of CRC cells.

Overexpression of JAML in CRC cells activated the PI3K-AKT-mTOR signalling pathway in vitro

Western blotting was used to verify the relationship between changes in JAML expression and the expression of PI3K, AKT, and mTOR in CRC cells (Fig. 4A). We found that after increasing JAML expression in DLD-1 and

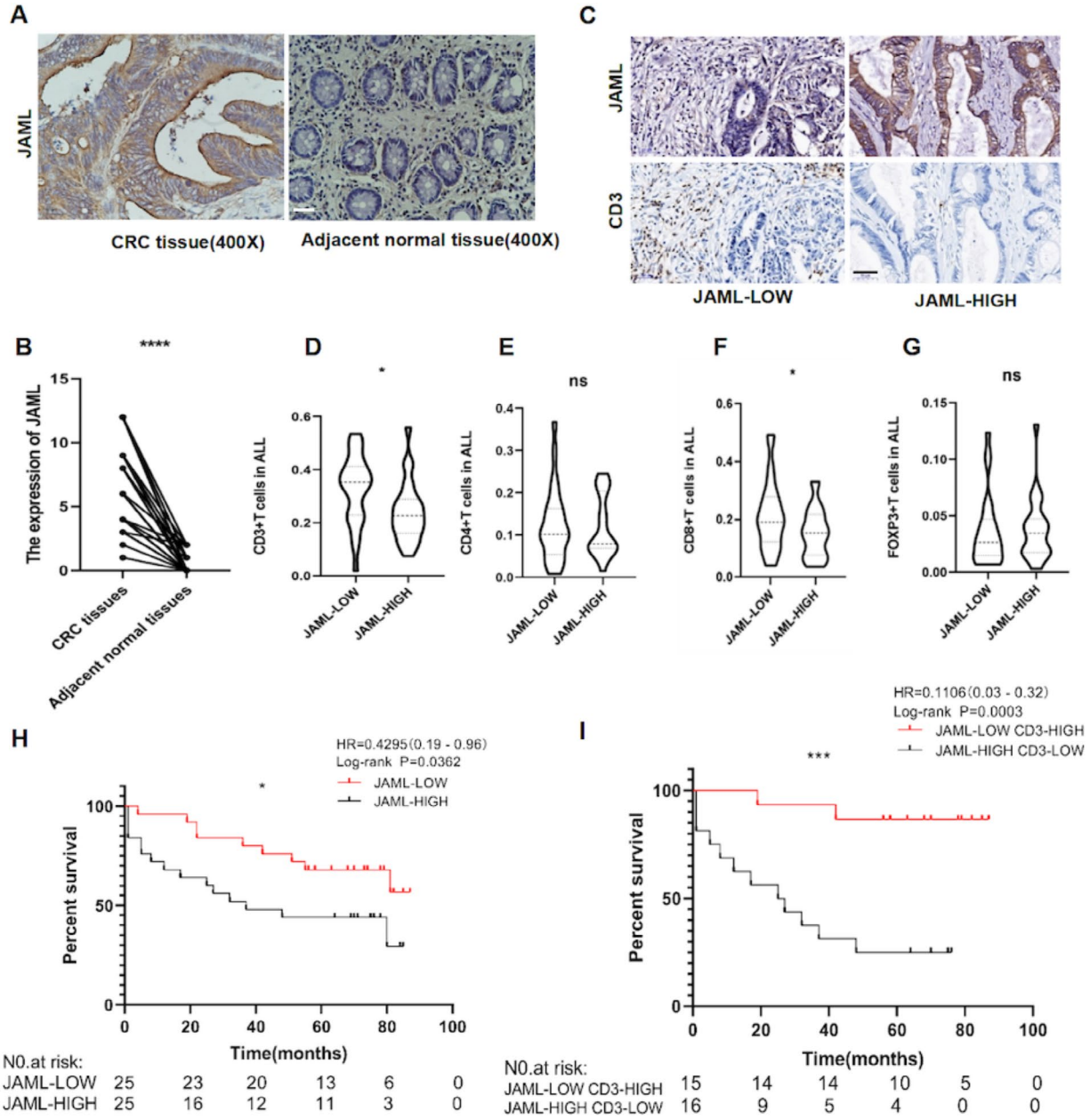

Fig. 1. (**A**) High expression of JAML was correlated with late TNM stage in patients with CRC, accompanied by decreased T-cell infiltration and poor prognosis. The expression of JAML in CRC tumor tissues (400x) and paracancerous tissues (400x); Brown staining showed positive JAML, which was expressed in the cytoplasm and membrane. (**B**) Quantitative analysis of JAML expression in CRC tumor tissue (n = 50) and paracancerous tissue (n = 50). (**C**) Images of $CD3^+$T-cell infiltration in tumor tissue with high JAML expression and tumor tissue with low JAML expression (400x). (**D**) Quantitative analysis of JAML expression and $CD3^+$T-cell infiltration density in tumor tissue. The density of tumor-infiltrating $CD3^+$T cells in the JAML-high group (n = 25) was lower than that in the JAML-low group (n = 25). (**E**–**G**) Quantitative analysis of JAML expression and the infiltration density of $CD4^+$T cells $CD8^+$T cells, and $Foxp3^+$T cells in tumor tissues. The infiltration density of $CD8^+$T-lymphocytes in the JAML-high patients (n = 25) was lower than that in the JAML-low patients (n = 25). (**H**) A high expression of JAML in CRC cells was related to worse OS. (**I**) Survival analysis showed that the OS in the $JAML^{-high}$-$CD3^{-low}$ subgroup was significantly lower than that in the $JAML^{-low}$-$CD3^{-high}$ subgroup.

Variables	JAML expression		
	High	Low	*p*
Age (year)			
≤60	9	11	0.564
>60	16	14	
Gender			
Male	16	12	0.254
Female	9	13	
Primary tumour			
T1-T2	1	1	1
T3-T4	24	24	
Regional lymph node involvement			
N0	8	21	0.00195
N+	17	4	
Histological grade			
G2	15	14	0.774
G3	10	11	
TNM stage groupings			
I-II	7	21	0.000066
III-IV	18	4	

Table 1. The relationship between the expression of JAML and various CRC pathological parameters.

SW480 cells, the expression of P-PI3K$^{TYR467/199}$, P-AKT^{SER473}, and P-mTOR^{Ser2448Ser2448} increased (Fig. 4B,C), whereas after reducing JAML expression in HCT116 and LOVO cells, the expression of P-PI3K, P-AKT^{SER473}, and P-mTOR^{Ser2448Ser2448} decreased (Fig. 4D,E). Next, we treated JAML-overexpressing DLD-1 and SW480 cells with the mTOR inhibitor rapamycin (Fig. 4F). The results of the Transwell migration and EdU proliferation assays showed that the migration and proliferation ability of DLD-1 and SW480 cells increased after JAML was overexpressed, while the increase in migration and proliferation caused by the overexpression of JAML was partially inhibited by the addition of the mTOR inhibitor (Fig. 4G–K). These results suggested that JAML promoted the migration and proliferation of CRC cells by activating the PI3K-AKT-mTOR signalling pathway in vitro.

Overexpression of JAML promoted the proliferation of CRC by activating the PI3K-AKT-mTOR signalling pathway in vivo

LOVO cells transfected with the JAML knockdown virus or control cells were subcutaneously inoculated into BALB/c nude mice, after which tumours were subcutaneously implanted and cultured. The tumour volumes of the mice were recorded regularly. The two groups of mice were sacrificed on the 40th day, after which the tumour tissue was weighed and embedded. After plotting the tumour growth curve, we found that the subcutaneous implanted tumours in the LOVO^{shJAML} group grew significantly more slowly than those in the control group did (Fig. 5A–D). We obtained tumour tissue sections from the mice and then performed IHC staining experiments. The results showed that in tumour tissues with low JAML expression, the expression of P-PI3K, P-AKT, and P-mTOR decreased significantly, while the expression of PI3K, AKT, and mTOR was similar in two groups (Fig. 5E–K). These results suggested that JAML promoted the proliferation of CRC by increasing the phosphorylation of PI3K-AKT-mTOR signalling pathway in vivo.

T-lymphocytes infiltration was reduced in tumour tissues with JAML high expression by decreasing chemokines

To verify the relationship between CRC-related JAML and tumour infiltrating lymphocytes (TILs) in the tumour immune microenvironment in vivo, we used MC38 cells to establish a CRC transplantation model in C57BL/6 mice. We also used lentivirus transfection to knockdown the expression of JAML in MC38 cells. MC38^{shJAML} cells and control cells were subcutaneously implanted into C57BL/6 mice after we obtained the corresponding MC38^{shJAML} cell line. We found that tumour growth in the MC38^{shJAML} group was significantly slower than that in the control group (Fig. 6A–D). We detected T-lymphocyte subsets in the tumour, by flow cytometry. As shown in Fig. 6E–G, downregulation of JAML in tumour cells significantly increased the proportion of CD8^{+}T cells in the tumour ($p < 0.05$). Immunohistochemical staining revealed that CD8^{+}T cells infiltration within tumour tissues increased significantly in MC38^{shJAML} group (Fig. 6H–K).

To clarify the mechanism by which JAML regulates the infiltration of T cells, we used transcriptome analysis, and we found that cytokine secretion was enriched in LOVO^{shJAML} cells (Fig. 6L). Subsequently, we used RQ-PCR to verify the relationship between JAML and the expression of various cytokines in CRC cells. The results showed that the expression of cytokines such as CCL2, CCL16, CCL20, CCL22, CXCL9, CXCL10 and CXCL11 increased when JAML decreased in LOVO cells (Fig. 6M). Similar results were observed for MC38 cells by RQ-

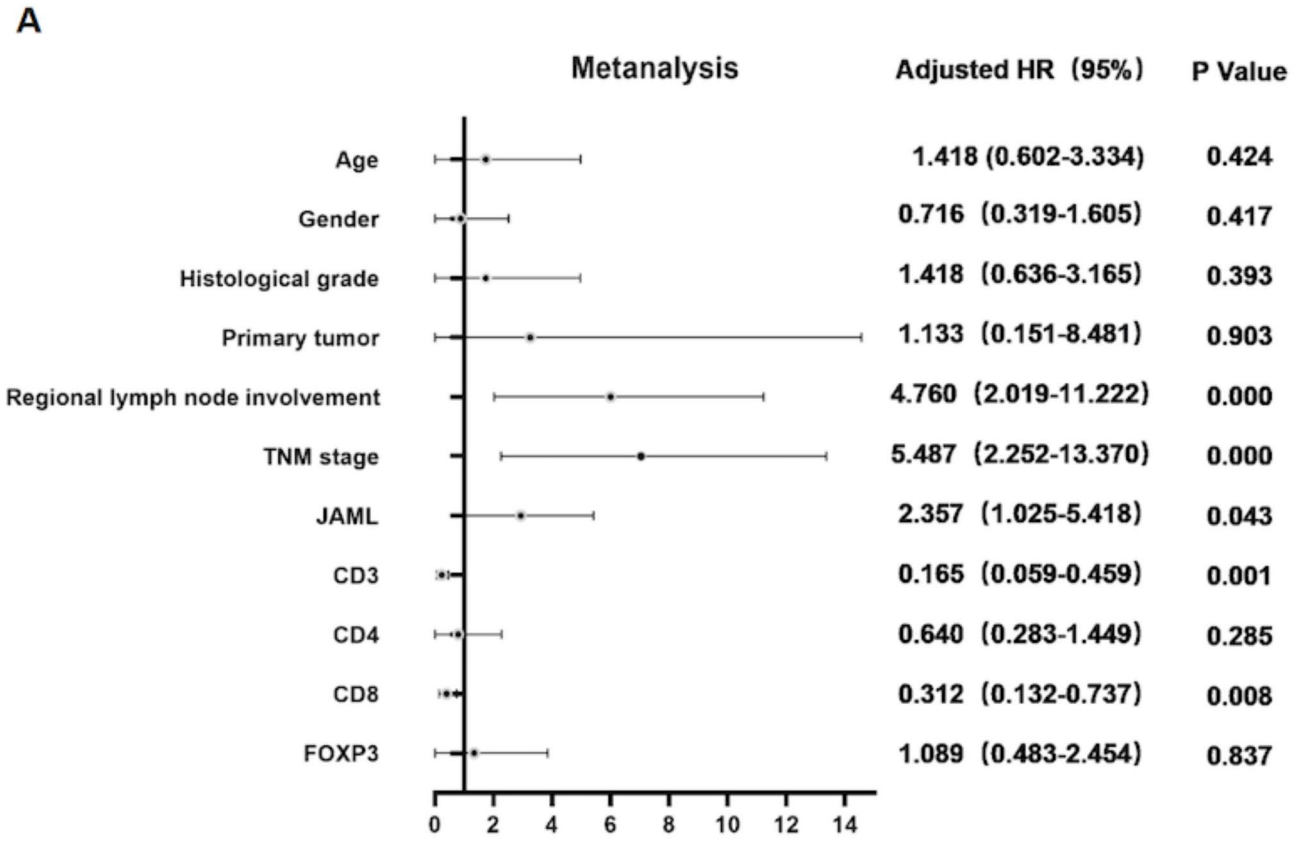

Fig. 2. Relationships between JAML and pathological parameters in patients with CRC. (**A**) CRC Mortality risk ratio analysis for each factor. The risk ratio and confidence interval (CI) of each factor for clinical prognosis were obtained through Cox univariate analysis. The forest plot was generated with GraphPad, with the horizontal line representing the 95% confidence interval and the circle dot representing the hazard ratio (HR).

PCR (Fig. 6N). After treatment with the mTOR inhibitor rapamycin, the expression of CCL20 and CXCL9/10/11 in LOVO and MC38 cells was upregulated significantly (Fig. 6O–R).

Discussion

After more than 20 years of translational and clinical investigations, targeting the anti-vascular endothelial growth factor pathway and anti-epidermal growth factor receptor pathway still represents the most relevant keystone for targeted molecular treatment of mCRC[3]. The survival of patients with mCRC has reached a plateau because of a lack of new strategies[1,16]. New therapeutic target is seriously important for patients with mCRC.

In this study, we found that JAML was highly expressed in patients with CRC, especially those with lymph node metastasis. Survival analysis revealed that high expression of JAML predicted poor survival in patients with CRC. These results were also supported by previous studies on gastric cancer and lung adenocarcinoma tissues[14,15]. However, our study also showed that the expression of JAML was not correlated with T stage in patients with CRC, which may have been due to the bias that almost all patients in our study had T3 or T4 disease. An ideal target for cancer therapy should be highly expressed in cancer tissues but poorly expressed in adjacent normal tissues, thereby minimizing off-target effects. Here, we report for the first time, from the basis of basic research, that JAML is highly expressed in CRC cells and promotes malignant biological behaviour in CRC cells, suggesting that JAML might be a promising therapeutic target for CRC.

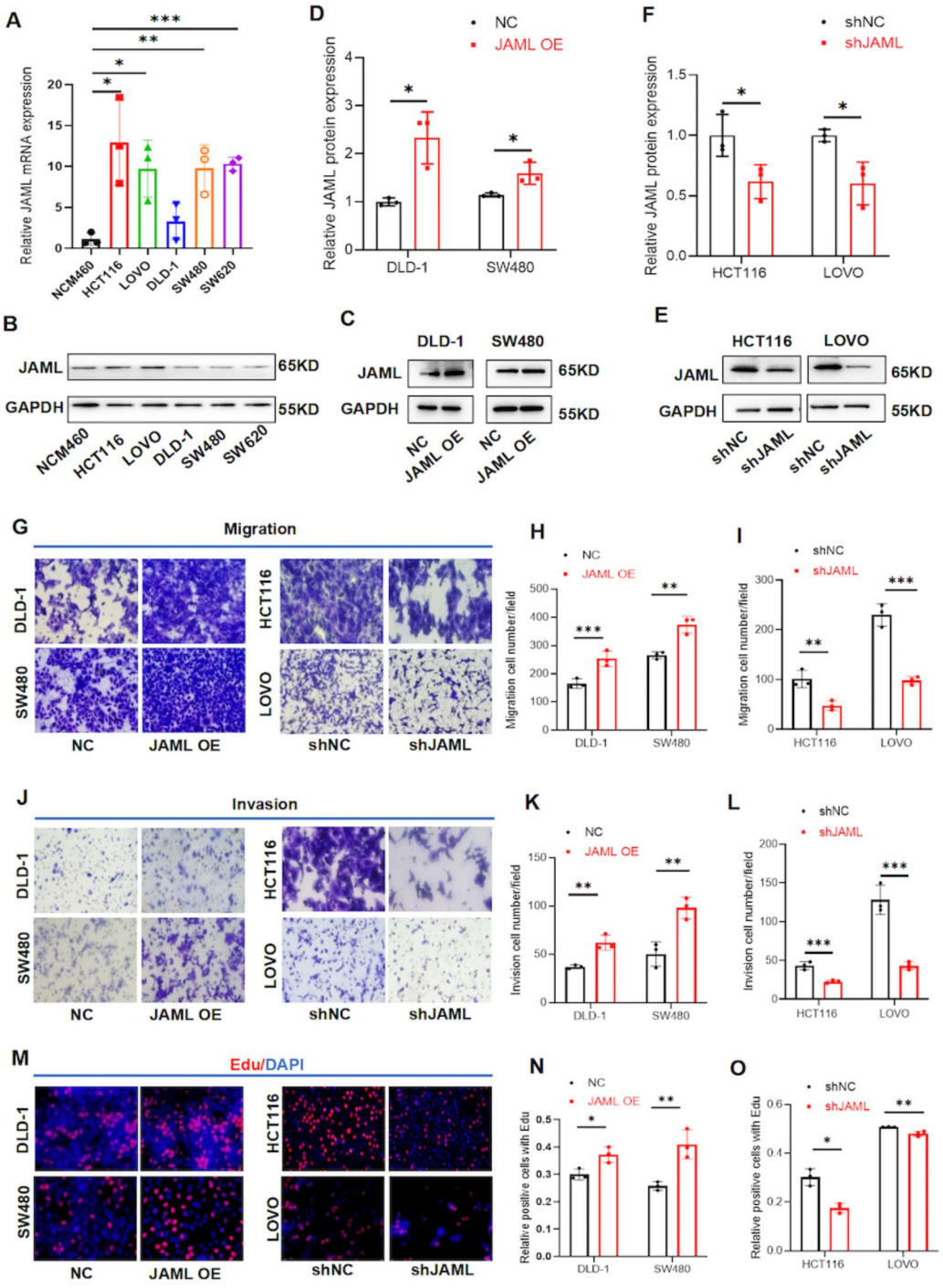

Fig. 3. JAML promoted the proliferation, migration, and invasion of CRC cells in vitro. (**A**,**B**) The expression of JAML in CRC cell lines (HCT116, LOVO, DLD-1, SW480, and SW620) and colorectal epithelial cells (NCM460). (**C**,**D**) Western blot analysis showed that the expression of JAML in DLD-1 and SW480 cells was significantly upregulated after transfection of the JAML plasmid. (**E**,**F**) Lentivirus transfection (shJAML) was used to transfect HCT116 and LOVO cells to reduce JAML expression. These results showed that the knockdown of shJAML3 was most effective. (**G**–**I**) Transwell migration and invasion experiments showed that overexpression of JAML significantly increased the migration and invasion of DLD-1 and SW480 cells. (**J**–**L**) Transwell migration and invasion experiments showed that low expression of JAML decreased the migration and invasion ability of HCT116 and LOVO cells. (**M**–**O**) The results of the EdU proliferation assay showed that overexpression of JAML significantly increased the proliferation ability of DLD-1 and SW480 cellsand low expression of JAML decreased the proliferation ability of HCT116 and LOVO cells.

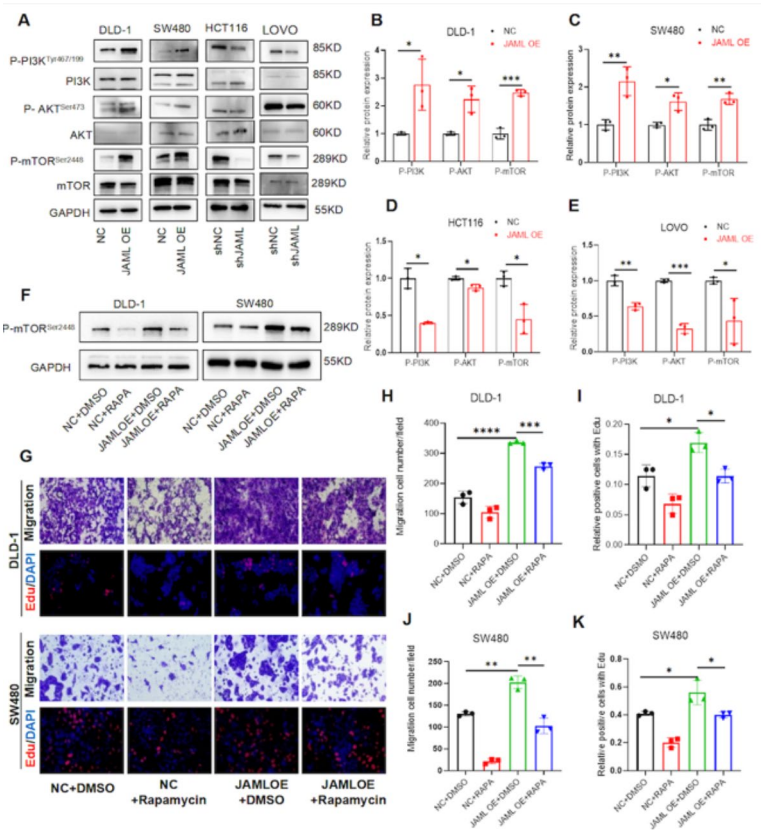

Fig. 4. JAML promoted the malignant biological behaviour of CRC cells by activating the PI3K-AKT-mTOR signalling pathway in vitro. (**A**–**E**) Western blotting results showing that after increasing JAML expression in DLD-1 and SW480 cells, the expression of P-PI3K$^{Tyr467/199}$, P-AKT^{Ser473}, and P-mTOR^{Ser2448} increased, whereas after reducing JAML expression in HCT116 and LOVO cells, the expression of P-PI3K$^{Tyr467/199}$, P-AKT^{Ser473}, and P-mTOR^{Ser2448} decreased. (**F**) P-mTOR^{Ser2448} expression increased after JAML overexpression in DLD-1 and SW480 cells, while P-mTOR^{Ser2448} upregulation by JAML overexpression was partially suppressed after rapamycin treatment. (**G**–**K**) The results of the Transwell migration assay and EDU proliferation assay showed that the migration and proliferation ability of cells increased after the overexpression of JAML in DLD-1 and SW480 cells, while the increase in migration and proliferation caused by the overexpression of JAML was partially inhibited by the addition of the mTOR inhibitor.

PI3K-Akt-mTOR is a key kinase activated by various cellular stimuli that controls the basic functions of cells, such as transcription, translation, survival, and proliferation. Dysregulation of the PI3K-Akt-mTOR pathway is known to drive cancer development and progression[17,18]. Our research showed that the PI3K-AKT-mTOR signalling pathway was activated in JAML high expressed CRC cells both in vitro and in vivo, promoting the proliferation, invasion, and migration of CRC. It was known that mTOR inhibitors such as rapamycin were the first PI3K-Akt-mTOR-targeting drugs to advance to the clinic. In our study, rapamycin reversed the malignant biological behaviour of JAML high expressed CRC cell lines. All these data showed that JAML promoted the proliferation, invasion, and migration of CRC through the PI3K-AKT-mTOR signalling pathway both in vitro and in vivo.

Immunotherapy leads to long-term survival and leads to innovation in patients with MSI-H/dMMR mCRC[19], however, the tumour tissues of patients with pMMR CRC exhibit insufficient recruitment of immune cells, leading to resistance to immune checkpoint inhibitors[20,21]. TILs participate in the formation of the tumour microenvironment, regulate local tumour immunity and are regarded as the most important part of the tumour immune microenvironment[22,23]. It has previously been proven that $CD8^+$ TILs are closely related to the efficacy of anti-PD-1/PD-L1 immunotherapy[24–26]. We found that high expression of JAML in cancer tissues was accompanied by decreased infiltration of T-lymphocytes, and poor survival in patients with CRC. And downregulation of JAML in MC38 cells increased the infiltration of $CD8^+$T-lymphocytes in C57BL/6 mice with normal immunity in vivo. Chemokines such as CCL20 and CXCL9/10/11 increased significantly after JAML was knocked down in CRC cells. It has been proved that CCL20 and CXCL9/10/11 can recruit T cells to cancer tissues and increase the efficacy of immunotherapy[27,28], partly confirming our findings. Targeting JAML might reverse resistance to immune checkpoint inhibitors in patients with mCRC.

All the clinical samples in our study were collected from postoperative specimens, which could not fully reflect the expression of JAML in metastatic colorectal cancer. Further studies should be conducted to clarify the mechanism of the relationship between the expression of JAML and the T-lymphocytes infiltration in mCRC.

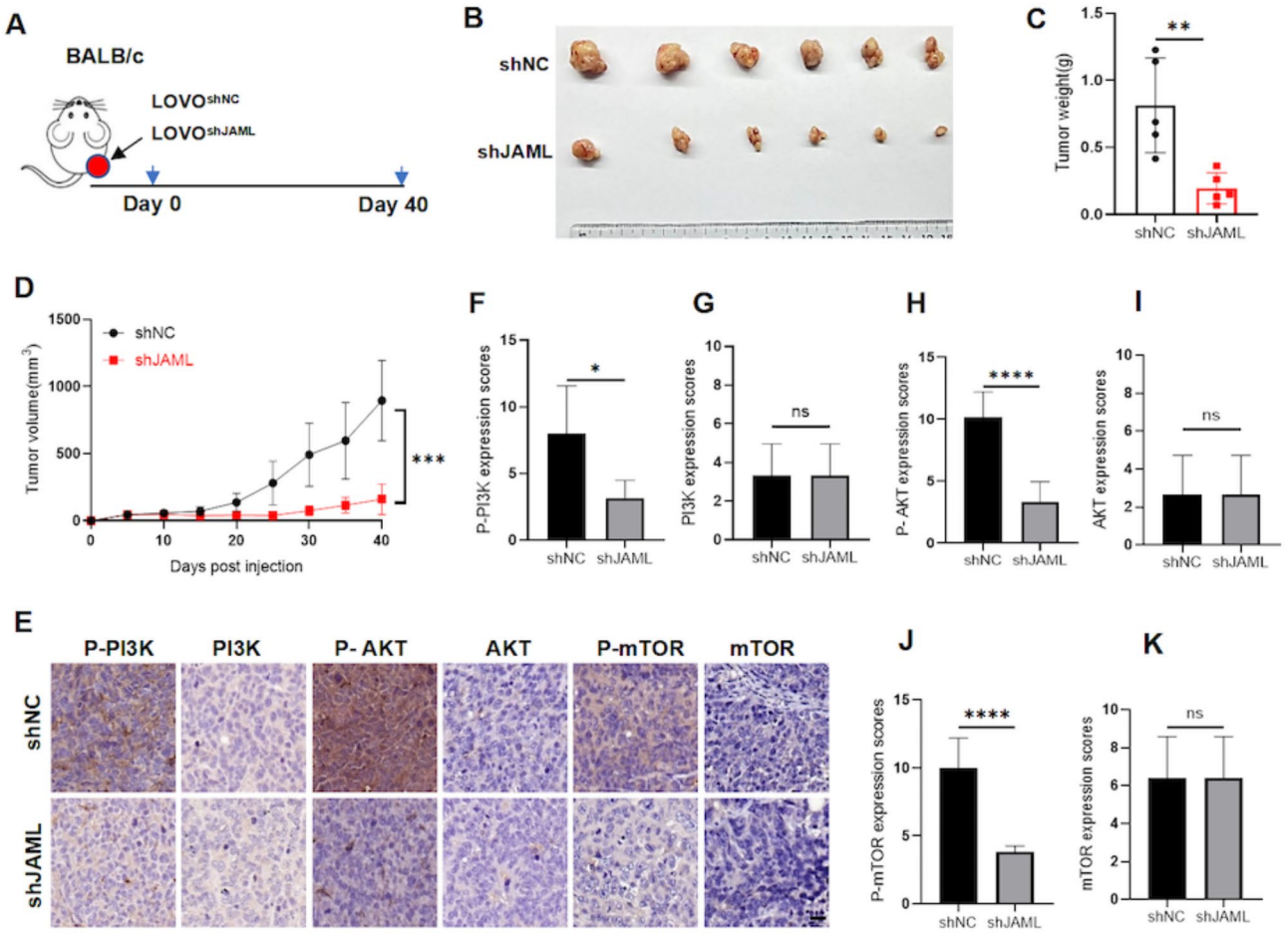

Fig. 5. JAML promoted CRC cell proliferation by activating the PI3K-AKT-mTOR signalling pathway in vivo. (**A**–**C**) LOVO cells transfected with the JAML knockdown virus or control cells were subcutaneously inoculated into BALB/c nude mice, after which tumours were subcutaneously implanted after culture. The tumour volumes of the mice were recorded regularly. The two groups of mice were sacrificed on the 40th day, after which the tumour tissue was weighed and embedded. (**D**) The tumour growth curve results showed that the subcutaneous implanted tumours in the LOVO^{shJAML} group grew significantly more slowly than those in the control group. (**E**–**K**) Immunohistochemical staining results showing that in tumour tissues with low JAML expression, the expression of P-PI3K$^{Tyr467/199}$, P-AKT^{Ser473} and P-mTOR^{Ser2448Ser2448} decreased.

In summary, we found that JAML was more highly expressed in CRC tissues than in adjacent normal tissues, especially in patients with late TNM stage. JAML overexpressed in CRC tissues was correlated with poor prognosis of patients. JAML promoted the proliferation, migration, and invasion of CRC cells by activating the PI3K-AKT-mTOR signalling pathway in vitro and in vivo, and reduced the infiltration of T-lymphocytes by downregulating the secretion of chemokines (Fig. 6). Our study ultimately identified JAML as a new target for cancer therapy, potentially providing a new strategy for patients with CRC.

Methods

Patient tumour samples

Paraffin tissue samples from 50 patients with colorectal cancer and adjacent normal tissues were collected from the Jinan Central Hospital Affiliated to Shandong First Medical University. The diagnoses were confirmed by postoperative pathological reports from January 2013 to December 2015. All patients were newly diagnosed with colorectal adenocarcinoma, but none of them had received chemotherapy, radiotherapy, targeted therapy,

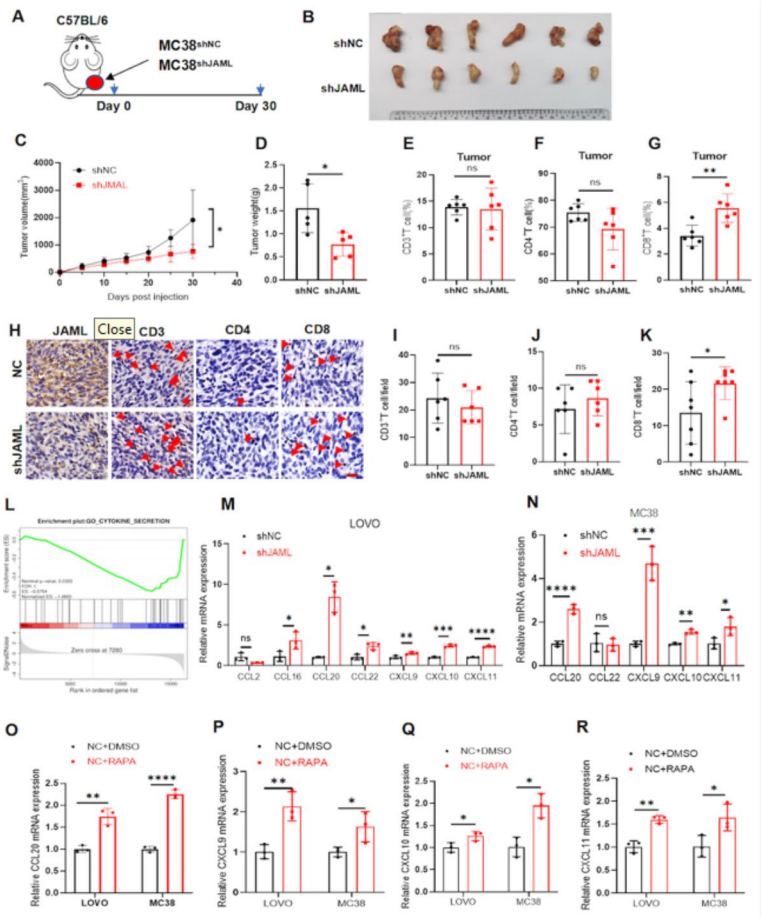

Fig. 6. T-lymphocytes infiltration was inhibited in tumour tissues with JAML high expression by decreasing chemokines. (**A**,**B**) MC38^{shJAML} cells and control cells were subcutaneously implanted into C57BL/6 mice, and tumours were subcutaneously implanted after culture. The tumour volumes of the mice were recorded regularly. The two groups of mice were sacrificed on the 30th day, after which the tumour tissue was weighed and embedded. (**C**,**D**) The tumour growth curve and weight of tumours in mice results showed that tumour growth in the MC38^{shJAML} group was significantly slower than that in the control group. (**E**–**G**) The immune cell subsets in the tumour were detected by flow cytometry. The results showed that knocking down JAML increased the proportion of CD8^{+}T cells in the tumour. (**H**) Transcriptome analysis showing enrichment of the expression of various cytokines when JAML was knocked down in LOVO cells. (**I**) RT-PCR results showing that the expression of cytokines such as CCL2, CCL16, CCL20, CCL22, CXCL9, CXCL10 and CXCL11 increased when JAML was decreased in LOVO cells. (**J**) The expression of cytokines such as CCL20, CXCL9, CXCL10 and CXCL11 increased when JAML was decreased in MC38 cells according to RT-PCR in vitro. (**K**–**N**) After treatment with the mTOR inhibitor rapamycin, the expression of CCL20 and CXCL9 in LOVO and MC38 cells was upregulated significantly.

or immunotherapy before surgery. Additionally, no other malignancies or metastases were detected here. Patients were classified according to the UICC/AJCC colorectal cancer Staging Criteria (8th edition).

Tumour cell lines

The human CRC cell lines HCT116, LOVO, DLD-1, SW480, and SW620 were all purchased from the Cell Resources Center, Chinese Academy of Sciences, Beijing, China. Human colorectal epithelial cells (NCM460) were purchased from the American Type Culture Collection (Manassas VA, USA). Additionally, the lentiviruses used for JAML overexpression and knockdown were purchased from GeneCopoeia. NCM460, LOVO, DLD-1, SW480, and SW620 cells were cultured in RPMI-1640 medium supplemented with 10% foetal bovine serum and 1% penicillin–streptomycin. Furthermore, HCT116 and HT29 cells were cultured in Dulbecco's modified DMEM supplemented with 10% foetal bovine serum and 1% penicillin–streptomycin. All the cells were cultured at 37 °C in a 5% CO_2 cell incubator.

Construction of stable cell lines

Stable strains were transfected with lentiviruses from cells in good condition or after more than 2 generations of resuscitation. After cell digestion and centrifugation, the cells were resuspended to a final cell concentration

of 3–5 × 10^4/ml. Two millilitres were then added to each well of a six-well plate. The next day, fresh lentivirus medium containing JAML-overexpression/knockdown cells was added to each well. The cell state was then observed after 4, 8, 12, and 16 h. If the cell deformation worsened, the fluid was changed immediately. After 48 h, the transfection efficiency was assessed using fluorescence microscopy. The transfection efficiency was then expressed as the percentage of living cells with green fluorescent protein (GFP). After 72 h, culture medium containing puromycin was added for 5 days to improve the efficiency of overexpression or knockdown. In the future, fluorescence microscopy should also be used to ensure that the cells transfected with viruses account for more than 80–90% of the experiments. If the transfection efficiency was low, culture medium containing puromycin was used to screen the cells.

Immunohistochemical (IHC) staining and quantification

The repaired wax blocks were sliced on a paraffin slicer to a thickness of 3 μm. IHC staining was conducted according to the instructions of the following kits: anti-JAML (Affinity, Cat No. DF2551), anti-CD3 (MXB Biotechnologles, Cat No. MAB-0740), anti-CD4 (MXB Biotechnologles, Cat No. RMA-0620), anti-CD8 (MXB Biotechnologles, Cat No. RMA-0514), and anti-Foxp3 (Abcam, Cat No. ab215206), and anti-CCL20 (Affinity, Cat No. DF2238).

Five visual fields were randomly intercepted from each slide under 200 × and 400 × magnification and evaluated by two separate researchers. The samples were subsequently scored according to the intensity and area of staining, with the results representing the expression intensity of the molecule in the tissue. The dyeing area was scored as follows: < 5% was scored as 0, 5–25% was scored as 1, 26–50% was scored as 2, 51–75% was scored as 3, and 76–100% was scored as 4. The dyeing intensity was scored as 0 for colourless, 1 for light yellow, 2 for brown, or 3 for brown. The final results were the product of the dye area and intensity fractions. A score of 3 points or less indicated no expression, 4 points or above indicated expression, 6 points or below indicated low expression, and 8 points or above indicated high expression.

RNA extraction and real-time fluorescence quantitative polymerase chain reaction (RQ-PCR)

Cell RNA was extracted using the Feijie RNA Rapid Extraction Kit and the RNAfast200 RNA Extraction Kit (Fastagen, Cat No. RNAfast200). The concentration of RNA was measured, and the quality of the RNA was determined according to the A260/A280 ratio. The reaction system was configured according to the RNA concentration. The mixture was subsequently placed into a reverse transcription metre, after which the temperature and duration of the reaction were set. The corresponding volumes of SYBR (AG; Cat No. AG11728), the upstream and downstream primers, and water were mixed in eight rows. After centrifugation, the samples were placed in a real-time PCR instrument. The relative expression of JAML and GAPDH was analysed and calculated by comparing the Ct values. All the experiments were performed in triplicate. The primers used in this study are listed in Supplementary table 1.

Western blot analysis

The cells were lysed with RIPA buffer containing proteolytic enzymes and phosphatase inhibitors. After determining the protein concentration of the cell lysis products using a BCA protein analysis kit, 20 μg protein samples were separated on a 10% sodium dodecyl sulfate-polyacrylamide gel and then transferred to a PVDF membrane. The membrane was then blocked in a 5% degreasing emulsion for 1 h before being incubated with the corresponding primary antibody overnight at 4 °C. The primary antibodies used were anti-JAML (1:1000, Abcam, Cat No. ab183714), anti-phospho-PI3K (1:1000, Abmart, Cat No. T40065), anti-PI3K (1:1000, Abmart, Cat No. T40064), anti-phospho-AKT (1:1000, Cell Signaling Technology, Cat No. 4060), anti-AKT (1:1000, Cell Signaling Technology, Cat No. 3285), anti-phospho-mTOR (1:1000, Cell Signaling Technology, Cat No. 2976), anti-mTOR (1:1000, Cell Signaling Technology, Cat No. 2983), anti-GAPDH (1:20,000, Proteintech, Cat No. 60004-1), HRP-labelled goat anti-rabbit secondary antibodies (1:5000, Origene, Cat No. ZB2301), and HRP-labelled goat anti-mouse secondary antibodies (1:5000, Boster, Cat No. BA1050). Subsequently, the PVDF membranes were washed and incubated with goat anti-rabbit or rat secondary antibodies conjugated with horseradish peroxidase. The bands were then visualized using an enhanced chemiluminescence (ECL) detection reagent, while tubulin was used as a loading control. All the experiments were performed in triplicate.

Cell proliferation experiments

An EdU (5-acetyne-2'-deoxyuridine nucleoside) DNA cell proliferation kit (Abbcine, Cat No. KTA2031) was used for the cell proliferation assays. After treatment with the required drug or other stimulants, measurements were conducted according to the operational requirements of the kit. A Nikon fluorescence microscope was used to observe and capture images. All the experiments were performed in triplicate.

Transwell invasion and migration experiments

Cell migration was measured using a polycarbonate film with an 8-mm aperture in a 24-well plate. The matrigel matrix was mixed proportionally with the base medium. Next, 100 μL of the mixture was added to each chamber. After the cells had been treated with the necessary drugs or other stimuli, they were digested and then suspended, after which the cell density was adjusted to 5 × 10^5/ml. Subsequently, 100 μL of the mixed cell suspension was added to the chamber before being incubated at 37 °C. After 24 h of culture, the cells were fixed and stained with crystal violet. Unmigrated cells in the upper chamber were wiped with a cotton swab, dried slightly, and then observed under an optical microscope (Nikon). Three visual fields were selected randomly for cell counting. All the experiments were performed in triplicate. This procedure was the same as that used for the Transwell invasion experiment, except that the substrate was not used here.

Animal experiments

BALB/c nude and C57BL/6 mice (6–8 weeks old) were purchased from Beijing Vital River Laboratory Animal Technology Co., Ltd (Beijing, China). Female BALB/c mice aged 6–8 weeks were selected for subcutaneous tumour transplantation. LOVO cells infected with the JAML knockdown/control lentivirus were prepared before being digested until the cells had grown to 70–80%, centrifuged, and precooled for washing thrice with PBS. The cell density was adjusted to 10^8/ml by resuspension in PBS. The cells were then injected into the lateral abdomen of the mice using a 1 ml sterile syringe. Tumour size was measured every 3 days. When the longest diameter of the tumour reached 2 cm, the tumours were separated and weighed. The expression levels of PI3K, AKT, and T-mTOR were detected via IHC staining after paraffin embedding. Mice were housed at 25 °C, 12 h light/dark and were euthanized using an overdose of anesthesia with 1–1.5% isoflurane, followed by exsanguination and tissue removal.

In addition, female C57BL/6 mice and MC38 cells were used to establish another subcutaneous tumour transplantation model via a similar method. When the mice were sacrificed, the tumours were separated for flow cytometry. The expression of CD3, CD4, CD8, and CCL20 in the tumour tissues was detected by IHC staining after paraffin embedding.

Flow cytometry analysis

Cells from the tumours of the mice were added to 3 ml of erythrocyte lysate and then incubated at room temperature. After 10 min, the supernatant was centrifuged at 1700 rpm, after which the solution was discarded. After the cells were washed for 5 min and centrifuged at 1700 rpm for 10 min, the lymphocytes obtained from tumour tissues were mixed with cellular stimulants and then incubated at 37 °C and 5% CO2 for 6 h, while the flow cytometry was used to detect CD3 (BioLegend, Cat No. 100204), CD4 (BioLegend, Cat No. 100434), CD8 (BioLegend, Cat No. 100712), and CD45 (BioLegend, Cat No. 103116) flow cytometry antibodies. The stained cells were subsequently analysed by FACS Calibur flow cytometry (BD Bioscience), while the data were analysed using FlowJo10 software (Tree Star, Inc.; Ashland, OR, USA).

mRNA sequencing

Cell RNA was extracted using the Feijie RNA Rapid Extraction Kit and the RNAfast200 RNA Extraction Kit (Fastagen, Cat No. RNAfast200). The RNA was stored at − 80 °C and subsequently transported to BGI for mRNA sequencing on dry ice. Sequencing was started after the samples passed quality control.

Statistical methods

All patients were followed up by telephone to obtain survival data. The final follow-up date was August 20, 2021. GraphPad Prism software (version 8.0) and SPSS Statistics were used for data analysis. We conducted normality tests on the data and employed the T-test to compare differences between two groups for data that conformed to a normal distribution. For data that did not conform to a normal distribution, we utilized the unpaired *t* test to determine whether significant differences existed between the two groups. The chi-square test was used to analyse the associations between JAML and clinicopathological parameters. The total survival time of all patients (measured in months) was obtained via telephone follow-ups and access to hospitalization data. Survival analysis was performed using log-rank and Kaplan–Meier survival curves. *, $p < 0.05$; **, $p < 0.01$; ***, $p < 0.001$; ****, $p < 0.0001$.

Data availability

The datasets generated and analysed during the current study are not publicly available but are available from the corresponding author on reasonable request.

Received: 23 April 2024; Accepted: 3 October 2024
Published online: 18 October 2024

References

1. Siegel, R. L., Miller, K. D., Wagle, N. S. & Jemal, A. Cancer statistics, 2023. *CA Cancer J. Clin.* **73**, 17–48 (2023).
2. Sinha, R. Colorectal cancer. *Clin. Radiol.* **76**, 870 (2021).
3. Ciardiello, F. et al. Clinical management of metastatic colorectal cancer in the era of precision medicine. *CA Cancer J. Clin.* **72**, 372–401 (2022).
4. De Falco, V. et al. How we treat metastatic colorectal cancer. *ESMO Open* **4**, E000813 (2020).
5. Stintzing, S. et al. Folfiri plus cetuximab versus folfiri plus bevacizumab for metastatic colorectal cancer (Fire-3): A post-hoc analysis of tumour dynamics in the final ras wild-type subgroup of this randomised open-label phase 3 trial. *Lancet Oncol.* **17**, 1426–1434 (2016).
6. Venook, A. P. et al. Effect of first-line chemotherapy combined with cetuximab or bevacizumab on overall survival in patients with kras wild-type advanced or metastatic colorectal cancer: A randomized clinical trial. *JAMA* **317**, 2392–2401 (2017).
7. Bando, H., Ohtsu, A. & Yoshino, T. Therapeutic landscape and future direction of metastatic colorectal cancer. *Nat. Rev. Gastroenterol. Hepatol.* **20**, 306–322 (2023).
8. Diaz, L. A. Jr. et al. Pembrolizumab versus chemotherapy for microsatellite instability-high or mismatch repair-deficient metastatic colorectal cancer (Keynote-177): Final analysis of a randomised, open-label, phase 3 study. *Lancet Oncol.* **23**, 659–670 (2022).
9. Eng, C. et al. Atezolizumab with or without cobimetinib versus regorafenib in previously treated metastatic colorectal cancer (Imblaze370): A multicentre, open-label, phase 3, randomised. *Controlled Trial. Lancet Oncol.* **20**, 849–861 (2019).
10. Gou, M. et al. Fruquintinib in combination with Pd-1 inhibitors in patients with refractory non-Msi-H/Pmmr metastatic colorectal cancer: A real-world study in China. *Front. Oncol.* **12**, 851756 (2022).
11. Moog-Lutz, C. et al. Jaml, a novel protein with characteristics of a junctional adhesion molecule, is induced during differentiation of myeloid leukemia cells. *Blood* **102**, 3371–3378 (2003).
12. Alvarez, J. I. et al. Jaml mediates monocyte and Cd8 T cell migration across the brain endothelium. *Ann. Clin. Transl. Neurol.* **2**, 1032–1037 (2015).

13. Zen, K. et al. Neutrophil migration across tight junctions is mediated by adhesive interactions between epithelial coxsackie and adenovirus receptor and a junctional adhesion molecule-like protein on neutrophils. *Mol. Biol. Cell* **16**, 2694–2703 (2005).
14. Fang, Y. et al. Junctional adhesion molecule-like protein promotes tumor progression and metastasis via P38 signaling pathway in gastric cancer. *Front Oncol* **11**, 565676 (2021).
15. Wu, Q. et al. Junctional adhesion molecule-like protein promotes tumor progression via the Wnt/B-catenin signaling pathway in lung adenocarcinoma. *J. Transl. Med.* **20**, 260 (2022).
16. Sung, H. et al. Global cancer statistics 2020: Globocan estimates of incidence and mortality worldwide for 36 cancers in 185 countries. *CA Cancer J. Clin.* **71**, 209–249 (2021).
17. Aoki, M. & Fujishita, T. Oncogenic roles of the Pi3k/Akt/Mtor axis. *Curr. Top. Microbiol. Immunol.* **407**, 153–189 (2017).
18. Ersahin, T., Tuncbag, N. & Cetin-Atalay, R. The Pi3k/Akt/mtor interactive pathway. *Mol. Biosyst.* **11**, 1946–1954 (2015).
19. Andre, T. et al. Health-related quality of life in patients with microsatellite instability-high or mismatch repair deficient metastatic colorectal cancer treated with first-line pembrolizumab versus chemotherapy (Keynote-177): An open-label, randomised, phase 3 trial. *Lancet Oncol.* **22**, 665–677 (2021).
20. Joyce, J. A. & Fearon, D. T. T cell exclusion, immune privilege and the tumor microenvironment. *Science* **348**, 74–80 (2015).
21. Philip, M. & Schietinger, A. Cd8(+) T cell differentiation and dysfunction in cancer. *Nat. Rev. Immunol.* **22**, 209–223 (2022).
22. Franchina, D. G., He, F. & Brenner, D. Survival of the fittest: Cancer challenges T cell metabolism. *Cancer Lett.* **412**, 216–223 (2018).
23. Kumar, B. V., Connors, T. J. & Farber, D. L. Human T cell development, localization and function throughout life. *Immunity* **48**, 202–213 (2018).
24. Fitzgerald, A. A. et al. Dpp inhibition alters the Cxcr3 axis and enhances Nk and Cd8+ T cell infiltration to improve anti-Pd1 efficacy in murine models of pancreatic ductal adenocarcinoma. *J. Immunother. Cancer* **9**, E002837 (2021).
25. Kumagai, S., Koyama, S., Itahashi, K., Tanegashima, T., Lin, Y. T., & Togashi, Y., et al. Lactic acid promotes Pd-1 expression in regulatory T cells in highly glycolytic tumor microenvironments. *Cancer Cell* **40**, 201–218 (2022).
26. Barry, M. & Bleackley, R. C. Cytotoxic T lymphocytes: all roads lead to death. *Nat. Rev. Immunol.* **2**, 401–409 (2002).
27. Kawanabe-Matsuda, H. et al. Dietary lactobacillus-derived exopolysaccharide enhances immune-checkpoint blockade therapy. *Cancer Discov.* **12**, 1336–1355 (2022).
28. Cui, Y. et al. Activation of melanocortin-1 receptor signaling in melanoma cells impairs T cell infiltration to dampen antitumor immunity. *Nat. Commun.* **14**, 5740 (2023).

Acknowledgements

This study was supported by the Natural Science Foundation of Shandong Province (ZR2022LSW006) and Beijing Science Development Fund (KC2021-JX-0186-68).

Author contributions

Research designation: Meili Sun. Experiment performance and data analyses: Yuying Fang, Yanan Liu, Zhilin Dong, Xinchao Zhao, Mingyan Zhang, Yawen Zheng, Chunsheng Yang, Yufeng Wang, Ning Liu, Peng Yan, Fei Yang, and Yan Zheng. Figure preparation: Yuying Fang, Yanan Liu, and Yuan Ma. Manuscript writing: Yuying Fang, Meili Sun, Yanan Liu, Yawen Zheng, Wencheng Zhang, and Jianmin Yang.

Declarations

Competing interests

The authors declare no competing interests.

Ethics statement

This study was approved by the Ethics Committee of the Jinan Central Hospital (JNCHIACUC2021-55). It followed their Standard Operating Procedures ensuring compliance with the principles of Good Clinical Practice and the Declaration of Helsinki and any applicable regulatory requirements. Written informed consent was obtained from all the participants. All animal experiments were approved by the Ethical Committee for Laboratory Animal Welfare, Jinan Central Hospital (JNCH2021-136) and complied with the ARRIVE guidelines and the National Institutes of Health guide for the care and use of laboratory animals (NIH Publications No. 8023, revised 1978).

Additional information

Supplementary Information The online version contains supplementary material available at https://doi.org/10.1038/s41598-024-75180-z.

Correspondence and requests for materials should be addressed to M.S.